Journal of Population Therapeutics & Clinical Pharmacology

RESEARCH ARTICLE
DOI: 10.53555/jptcp.v31i2.4594

EXPLORING THE ANTI-CERVICAL CANCER POTENTIAL OF *CASSIA ANGUSTIFOLIA*: INSIGHTS FROM HELA CELL LINE, AND MOLECULAR DOCKING

Aasia Kalsoom[1]*, Awais Altaf[2]*, Tahir Maqbool[3]*, Saira Aftab[4], Huma Sattar[5], Muhammad Sajjad[6], Asia Kiran[7]

[1*,2*,3*,5,7]Institute of Molecular Biology and Biotechnology (IMBB/CRiMM), The University of Lahore, Lahore, Pakistan, Emails: asiyakalsoom0608@gmail.com (Aasia Kalsoom); awaisaltaf362@yahoo.com (Awais Altaf); tahir.maqbool@imbb.uol.edu.pk (Tahir Maqbool); huma_48biotech@yahoo.com (Huma Sattar); asiakiran8@gmail.com
[4]Department of Biochemistry and Biophysics, Stockholm University, Stockholm, Sweden Email: saira.aftab@dbb.su.se
[6]School of Biological Sciences, Punjab University, Lahore, Pakistan, Email: Sajjad.sbs@pu.edu.pk

***Corresponding Authors:** Aasia Kalsoom, Awais Altaf, Tahir Maqbool
*Institute of Molecular Biology and Biotechnology (IMBB/CRiMM), The University of Lahore, Lahore, Pakistan, Emails: asiyakalsoom0608@gmail.com

Abstract
Cassia angustifolia (CA: senna makkai) is a medicinal plant that belongs to Saudi Arabia and Egypt and is widely cultivated in Pakistan. This study was designed for the *in vitro* anticancer assessment of *Cassia* extracts on cervical (HeLa) cancer and noncancer human embryonic kidney (HEK-293T) cell lines. The MTT (3-(4,5-Dimethylthiazol-2-yl)-2,5-Diphenyltetrazolium Bromide) and crystal violet assays were performed to determine the cytotoxicity of extracts. For the mRNA expression analysis of *p53* and *Bcl2*, the SYBR Green-based Real-time PCR was performed. Molecular interaction analysis and binding affinity were explored between target proteins (TP53, BCL2, EGFR, and HER2) and compounds through computational approaches. GCMS was used to identify the phytocompounds with anticancer potential using ethanol (ECA) and n-hexane (HCA) solvent systems. GCMS analysis showed the presence of bioactive phytochemicals in both CA extracts. These extracts demonstrated dose-dependent growth inhibition of tumor cells with an IC_{50} value of 50 and 76 µg/mL. Significant downregulation of *TP53* (tumor suppressor) and upregulation of the *BCL-2* (antiapoptotic) proteins was observed after treatment with CV extracts. Phenol, 2-methyl-5-(1,2,2-trimethylcyclopentyl)-, (S)- was observed as the most potential bioactive compound towards TP53 (-7.5) (kcal/mol) protein, followed by Isophytol (-6.9). This work highlights cancer-target proteins involved in proliferation and drug-like compounds for cervical cancer treatment. Based on all these findings, it is concluded that ECA extract has promising anticancer potential and might be valued for the advancement of novel plant-derived drugs for treating and managing cervical cancer.

Keywords: *Cassia angustifolia*, HeLa cell line, anticancer phytocompounds, gene expression, molecular docking

Introduction:

Natural compounds produced by plants have been seen as the most promising options for cancer treatments in recent years. With few harmful effects on healthy cells, they can selectively destroy tumor cells. Their negligible side effects, innate biological activity, structural complexity, and chemical variety are the main reasons for their use as therapeutic agents (Aung *et al*., 2017). Flavonoids, terpenoids, alkaloids, and phenols are among the various plant-derived organic compounds that have antitumor properties. These products can inhibit tumor cell progress, inhibit telomerase activity, regulate apoptosis, stop angiogenesis, enhance immunity, alter resistance-causing signaling, and more (Ouyang *et al*., 2014; Kikuchi *et al*., 2019). Now, radiotherapy, immunotherapy, locally targeted therapy, and surgical resection are the main cancer treatments. Traditional therapy works well for early-stage cancer, but because of significant side effects, drug resistance, numerous recurrences, and metastases, they are not as successful for cervical cancer that has progressed locally or metastatically (He *et al*., 2021).

Additionally, several side effects and drug resistance were observed with the commonly prescribed medications for cervical cancer (Federico *et al*., 2021). One of the most potent anticancer medications, cisplatin, could resist through a self-defense mechanism (Park *et al*., 2021). In patients with cervical cancer, 5-fluorouracil (5-FU) has also been shown to have side effects and resistance (Sun *et al*., 2014). For the treatment of cervical cancer, it is therefore necessary to create medications with a better safety profile and increased efficacy. Numerous active compounds in natural products derived from plants are considered appealing substitutes for chemotherapy medications or appropriate for usage in conjunction with chemotherapy medications (Momtazi-Borojeni *et al*., 2018). Purified flaxseed hydrolysate (PFH), for instance, which is isolated from Lignan, suppresses angiogenesis and metastasis in HeLa cells and initiates the induction of apoptosis (Ezzat *et al*., 2018). In SiHa and CaSki cells, *Nigella sativa* thymoquinone also exhibited antiproliferative and apoptotic effects. These natural compounds include ethanol extracts from Praeruptorin-B, and popular tea (Park *et al*., 2021). There were almost 342,000 deaths from cervical cancer in 2020, and 604,000 new cases worldwide have been reported, becoming the most recurrent cancer among women. In 2020, developing countries reported almost 90% of disease-diagnosed cases and deaths globally (Sung *et al*., 2021). HPV (human papillomavirus) is the most common sexually transmitted infection, and HPV infections are the primary cause of nearly all cervical malignancies (Kumari *et al*., 2021). The strongest indicator of an elevated risk of cervical cancer is a persistent, high-risk HPV infection; however, the expression of several other biomarkers of cell proliferation and apoptosis, such as *p53* and *Bcl-2*, are crucial in the pathophysiology of cervical cancer (Abhilashi *et al*., 2023). The *p53* gene, found on chromosome 17, encodes the cell cycle checkpoint protein p53, which is crucial for regulating apoptosis and cell proliferation. When cellular stress triggers an increase in p53 protein levels, *p53*-responsive genes are expressed differently, which leads to cell cycle arrest or even death. As stated by Abhilashi et al. (2023), *E6*, the HPV oncoprotein attaches to the p53 protein thereby inhibiting its apoptotic function in cervical cancer cells, eventually leading to uncontrolled cell division. Bcl-2 and Bax are the two most important apoptosis-controlling proteins in this family. As an antiapoptotic protein, BCL2 has a regulatory role in cell survival and proliferation by directly binding to BAX or preventing the activation of proapoptotic proteins (Salam *et al*., 2020). In this study, molecular docking has been performed to better understand the stability, flexibility, and density of protein-ligand interactions, as well as the ideal ligand-bound orientation. This study attempted to adapt computer-aided programs to combine biological and chemical domains to expedite the drug development process. We hypothesized that the natural anticancer chemicals found in this study would work well as substitutes for conventional chemotherapeutics that are frequently used in cancer therapy. This study assessed the anticancer activity of CA: *Cassia angustifolia* extracts in response to a human-derived 2D cervical cancer cell model and analyzed the differential expression of tumor suppressor and apoptosis regulatory genes (*TP53* and *BCL2*) to explore the complicated molecular mechanisms.

Experimental details:

Plant identification and formulation of ECA and HCA extracts:

CA leaves were collected from Lahore city and were approved (GC. Herb. Bot. 3908) by a taxonomist at Government College University, Lahore, Pakistan, and voucher specimens were deposited for future reference. The powdered material (300 g) was then soaked into 1.0 L of organic solvents (ethanol 90%, and n-hexane 95%) (Sigma-Aldrich) separately in flasks at 37 °C in a dark room for five days. Centrifugation was performed at 2000 rpm for 15 min and the supernatants were filtered. The filtrates were concentrated using a rotary machine (Heidolph Hei-Vap, Germany). Lyophilization (Freeze drying) yielded dried extracts and stored them in aliquots at 4 °C for further experiments (Sultana *et al*., 2022). Crude extracts were then subjected to GC-MS analysis.

Extract analysis:

Phytochemical identification using GCMS:

The lyophilized ethanol and n-hexane extracts of plant leaves were sent to the ICCBS center, HEJ, University of Karachi, Karachi, Pakistan, for gas chromatography-mass spectrometric (GC-MS) identification of bioactive phytocompounds.

The instrument containing an average DB 35 MS capillary and non-polar column having 30×250mm dimensions, a 7890 A GC system, and a Triple-axis detector were utilized in the GCMS having EI and CI ion source. Helium gas was used with a flow rate of 1.0 mL per minute. Further, the injector temperature was set at 250 °C, 300 °C for the interface, and 300 °C for injection temperature. The column temperature was fixed at 150 V at 4 °C/min. After that, it was increased to 250 °C, and then to 20 °C per minute and maintained there for five minutes. The comparative percent amount of compounds was resolute through the peak area of each component to the entire area. The MS software was utilized to collect the data. The HEJ GC-MS library and a comparison of their retention indices served as the foundation for the compound identification. The mass spectrum was examined using the NIST databank, which has over 62000 patterns. Comparing the spectra of known compounds with the NIST database made it easier to understand the molecular weight, mass spectrum, chemical formula, and name of various compounds.

Cancer cell cultivation:

Human-derived cervical cancer, namely HeLa and noncancer cell lines HEK-293T, were taken from the University of Lahore's cell BioBank (IMBB/CRiMM). Cancer cultures were grown in DMEM (Caisson Lot#02160032), comprising 10% fetal bovine serum (FBS) (Sigma-Aldrich Lot#BCBS3184V) supplementation, 100 U/mL of *Penicillin-Streptomycin* (Caisson Lot#10201011). On the other hand, the normal human kidney cells (HEK-293T) were cultivated in Minimum Essential Media (MEM). The cells were placed in an atmosphere containing 5% CO_2 at 37 °C. Slight modifications were made to the passage procedure after the cells reached 80% confluency. Following removing the medium, cells were cleaned with PBS solution (Inovatiqa Lot#153595), and trypsin (3 mL) (Gibco Lot#1297823) was added for separation, followed by observation under an inverted microscope. Cells were separated, centrifuged, and then plated in 96-well plates for additional tests. Complete media (5 mL) stopped the activity, and the cells were subjected to centrifugation at 1200 rpm for 7 min. Every 5 mL of cell aggregates was transferred to a T75cm^2 flask as part of the passage procedure (Masuku and Lebelo, 2019).

Treatment:

Four groups of triplicates received different treatments: 1st group, Untreated (UT, 2% FBS) to compare before and after treatment effects; 2nd group, DMSO (vehicle control: 0.1%) were taken as vehicle control; 3rd group, extract concentrations (ECA, and HCA) treated HeLa, and HEK-293T cells, 4th group; Cisplatin (10 µg/mL) (Receipt No, 651278) positive control of study. Further, 96 well plates for MTT and crystal violet and 6 well plates for mRNA expression analysis were done with applied IC_{50} concentrations by polymerase chain reaction.

Cell viability analysis:

In 9 mL of PBS, a crystal violet solution (0.1% WV) (Sigma-Aldrich) was added to make a working solution. With a few minor modifications, the crystal violet (CV) assay was carried out following the Nawaz et al. (2021) procedure. In a 96-well microtitre plate, HeLa, and HEK-293T cells were added (1×10^4 cells/well) in 200 µL of complete media. The incubation of 72 hrs was spent at the predetermined temperature of 37 °C with humidity and 5% CO_2. The cells were fixed with 70% ethanol for 10 minutes. After that, the CV solution (100 µL) was added to stain the cells and allowed to stay for 30 minutes. PBS was used to clear the cells from debris, and 200 µL of the triton X-100 solution (Sigma-Aldrich CAS#9036-195) was used to de-stain the cells. After 30 minutes of incubation at room temperature, the optical densities (OD) of samples at 570 nm were measured using a spectrophotometer (Nawaz *et al*., 2021). By using this formula we calculated the percentage of alive cells.

$$\text{Percentage viability} = \frac{\text{A570 of treated cells}}{\text{A570 of control cells}} \times 100$$

MTT analysis:

With the use of the 3-(4,5-dimethylthiazol-2-yl)-2,5-diphenyltetrazolium bromide (MTT) protocol, the cytotoxicity of plant extracts was assessed. In a nutshell, the cells underwent culture and treatment. Following a 200 µl complete medium incubation, a monolayer of cells was rinsed with PBS. Dimethyl sulfoxide (DMSO) (Invitrogen Inc., USA) was used to dissolve *C. angustifolia* crude ethanol and n-hexane extracts at a concentration of 160 mg/mL. A 96-well microtitre plate with 1×10^4 cells per well was obtained with seeding. ECA and HCA plant extracts were applied with 10, 50, 100, 200, and 400 µg/mL. The final stage was to incubate at the previously specified temperature with 5% CO_2. To perform the MTT assay, 25 µL of MTT component was added to every well, which was then left to incubate for 2 hrs. In living cells, the MTT turned to purple-colored formazan, which was then subjected to solubilization using 150 µL of dimethyl sulphoxide (DMSO) (Invitrogen Inc., USA). The media was removed, following the cellular growth was assessed under a microscope. Lastly, absorbance at 570nm was taken and IC_{50} values were calculated by applying the linear regression method (Kalsoom *et al*., 2023).

Morphological assessment of cancer and noncancer cells:

Using the Floid Cell Imaging Station, the morphological variations of HeLa, and HEK-293T cells were observed and compared to the control group to examine the impact of plant extracts on cancer and non-cancerous cell proliferation.

Real-time PCR study of P53 and BCL2 proteins in cervical cancer samples:

RNA extraction and cDNA synthesis:

New 6-well microtiter plates were used to culture HeLa cells (3×10^5) for further *in vitro* mRNA assessment. The concentration used in this test was based on a previously calculated IC_{50} value. After hrs, the concentration dose was applied and incubated for 72 hrs. On removing the media, PBS was used to wash the cells to remove debris (Mbugua *et al.,* 2019). HeLa cell RNA was extracted from the treated and untreated samples using a Pure Link RNA mini kit (CAT: 12183018A, Thermo Scientific, USA), as per the manufacturer's protocol. To estimate the concentration of RNA, 1 µL of the sample was used by Nanodrop (Thermo scientific ND 2000/2000c Spectrophotometers) at 260/280 nm, and the concentrations were obtained as ng/µL. The extracted RNA was stored at – 80 °C until processed for cDNA synthesis. cDNA synthesis was performed using extracted RNA following the manufacturer protocol (ABScript II cDNA First-Strand Synthesis Kit, Lot: 962100J09W09).

Real-time PCR analysis:

The area was amplified using real-time PCR (Qiagen Rotor-Gene Q 5plex HRM) along with forward and reverse primer sets. Primers were first used to amplify the synthesized cDNA using an absolute master mix that included buffer, Taq polymerase, and dNTPs mix. The qPCR conditions were set as follows: five minutes of initial denaturation at 95 °C, fifteen seconds of denaturation cycle time at 95 °C, annealing at 60 °C for 15 sec, and at 72 °C for fifteen minutes, followed by ten minutes of final extension at 72 °C. The primer annealing temperature for the second cycle of amplification was set for 40 seconds at 55 °C. The ΔCt values were calculated by subtracting the endogenous *Hprt1* gene's Ct value from the mean Ct values of the target genes *TP53* and *BCL2*. The ΔΔCt value was calculated by: ΔCt of sample-ΔCt of calibrator, and the fold change was measured using the formula $2^{-\Delta\Delta Ct}$ (Sattar *et al.*, 2021). The region to amplify *TP53*, *BCL2*, and *Hprt1* (reference) genes encompass a partial 5´ upstream region. Primer sequences were retrieved from NCBI and designed through the online software Primer3 (https://primer3.org/). All reactions were carried out three times, and primer sequences are shown in Table 1

TABLE 1: Details of primers designed and 'AZENTA' IDs.

Sr. No	Gene names	Primer sequence/ID	GC %	Tm (^{0}C)	BP	Size
1.	*TP53*-F	5´TTCGACATAGTGTGGTGGTG 3´ **ID:** S2052409355K	50	57.9	20	487
	TP53-R	5´CCCTTTTTGGACTTCAGGTG 3´ **ID:** S2052409356K	50	59.5	20	
2.	*BcL2*-F	5´GGGATTCCTGCGGATTGACA 3´ **ID:** S2052409351K	55	60	20	551
	BcL2-R	5´TCCCGGTTATCGTACCCTGT 3´ **ID:** S2052409352K	55	60	20	
3.	*Hprt1*-F	5´CGAACCTCTCGGCTTTCC 3´ **ID:** S2052409353K	60	60.8	18	455
	Hprt1-R	5´TCCCCTGTTGACTGGTCATT 3´ **ID:** S2052409354K	50	60.3	20	

Molecular docking:

Protein target prediction and preparation for cervical cancer treatment:

After searching the RCSB protein (URL: https://www.rcsb.org) data library, we obtained the x-ray crystallographic 3D structures of four target proteins, including P53, Bcl2, EGFR, and HER2 with PDB IDs: (2OCJ, 2W3L, 3poz, and 1n8z). Through the docking process, interactions took place with the possible disease-causing targets for CC therapy. The crystal structures of potential proteins were altered to add polar hydrogens, eliminate water molecules, remove heteroatoms along with the addition of polar hydrogen atoms and charges (Kollman & gasteiger charges), and save the prepared proteins in the PDBQT format. The active site amino acid residues and docked complexes were analyzed with PyMOL (version: 2.5.4, 2010, Shrodinger L.L.C.) (Kiran *et al*., 2023). The Autodock 4.2.6 software was used to configure the grid box to the co-crystalized ligand for docking, and dimensions were detailed in a config.txt format (Baeshen *et al*., 2022). The automated protein-ligand interaction profiler (PLIP) webserver was used to investigate the active residues participating in forming hydrogen as well as hydrophobic connections and the bond lengths observed between ligand and target proteins.

Ligand selection and preparation:

The structures of phytocompounds with anticancer potential were recovered from the PubChem (https://pubchem.ncbi.nlm.nih.gov) databank in an SDF format and further kept in PDB format using BIOVIA Discovery Studio Visualizer (Client 2021). The small molecules were arranged by independently uploading them into the autodock vina tool and saved in pdbqt format to run docking (Umesh *et al*., 2020).

Screening of compounds for drug-likeness:

Different computational tools were used to screen and calculate the physicochemical properties and pharmacokinetics of drug-like compounds. Following Lipinski's RO5 (Lipinski *et al*., 1997; Pillaiyar *et al*., 2020), factors including lipophilicity (LogP), hydrogen bond acceptors (nHBAs), and donors (nHBDs), molecular weight (MW), molar refractivity (MR), rotatable bonds (nRotBs) were find out using SwissADME (http://www.swissadme.ch/index.php). Following ADMET calculations, including BBB permeability, carcinogenicity, aqueous solubility, cytochrome P450 (CYP) enzymes, hepatotoxicity, toxicity, GI absorption, mutagenicity, and plasma drug clearance were predicted (Baeshen *et al*., 2022). For this purpose, the canonical SMILES of selected drug-like natural compounds were uploaded to the admetSAR (http://lmmd.ecust.edu.cn/admetsar2) website to examine their ADMET properties (Cankaya, 2020).

Molecular docking analysis using Autodock Vina:

AutoDock 4.2.6 was downloaded from 'The Scripps Research Institute's official website (http://autodock.scripps.edu/) (Ravindranath *et al*., 2015). The protein molecule that had been processed was fetched into the Auto Dock 4.2.6 workspace and subsequently utilized as the target after being saved in PDBQT format (Shivanika *et al*., 2020). After preparing the proteins and ligands for docking, the desired conformations were achieved by fixing the x, y, and z dimensions with a resolution of 0.500 Å (Table 2). Molecular docking of phytocompounds with less binding affinities and RMSD values (<1Å) showing stable interactions between ligand and target receptors was preferred. Different interactions including hydrophobic and hydrogen bonding, were analyzed using PLIP software (Umar et al., 2021). Biovia Discovery Studio client 2021 was used to take 2D and 3D images of docked complexes (Mendie and Hemalatha, 2022).

Table 2: Grid box dimensions for cervical cancer target proteins

Targets	Center			Size			Spacing	Exhaustiveness
	X	Y	Z	X	Y	Z		
TP53	20.681	19.971	14.415	40	40	40	0.775	8
BCL2	40.059	30.580	-5.437	40	40	40	0.481	8
EGFR	20.341	30.686	9.128	40	40	40	0.481	8
HER2	1.526	104.419	129.212	40	40	40	0.375	8

Data Analysis:

Every experiment was run three times. Through Graph Pad Prism 8.0, a one-way analysis of variance (ANOVA) and Tukey's test were applied. The proportion of variance in the result variable is represented by the R-squared statistics, which were obtained from analyses based on the general linear model (e.g., regression, ANOVA). The linear regression approach was used to determine IC_{50} values. A *p*-value of < 0.05 with a 95% confidence interval (CI) was considered statistically significant.

Results:

Total yield of crude extracts:

The total yield percentage of ECA extract was calculated as 16.35%, however, HCA yielded 15.64%. These extracts showed high yield determined by using the following formula: (Tulashie *et al*., 2021).

$$\text{Percentage yield (g)} = W1 \times 100 / W2$$

W1= Weight of extract residue
W2= Weight of powdered material

Profiling of phycompounds by GCMS:

A total of 26 and 30 compounds were profiled from ECA and HCA extracts of the leaves. GC-MS profiling of potential compounds by their peak area percentage, molecular formula (MF) and weight (MW), and retention time (RT). One of our earlier studies on *C. angustifolia* extracts reported the identified phytocompounds listed below **(Kalsoom *et al*., 2023)**

TABLE 2: GC-MS identified phytocompounds from *C. angustifolia* extracts

Sr No.	Compounds name	MF	Ethanol extract (ECA)			Hexane extract (HCA)		
			RT (min)	MW (g/mol)	Area %	RT (min)	MW (g/mol)	Area %
1.	Isoamyl acetate	$C_7H_{14}O_2$	7.6	130	0.29	7.7	130	0.71
2.	2,7,10-Trimethyldodecane	$C_{15}H_{32}$	10.6	212	0.32	-	-	-
3.	Octadecane	$C_{18}H_{38}$	13.5	254	0.66	-	-	-
4.	Ethyl alpha-d-glucopyranoside	$C_8H_{16}O_6$	14.9	208	1.73	-	-	-
5.	2,6,10-Trimethyltetradecane	$C_{17}H_{36}$	15.9	240	0.68	-	-	-
6.	3,7,11,15-Tetramethyl-2-hexadecen-1-OL	$C_{20}H_{40}O$	17.3	296	0.36	-	-	-
7.	7,9-Di-tert-butyl-1-oxaspiro[4.5]deca-6,9-iene-2,8-dione	$C_{17}H_{24}O_3$	18.4	276	0.95	-	-	-
8.	Palmitic acid	$C_{16}H_{32}O_2$	18.9	256	6.03	-	-	-
9.	Ethyl palmitate	$C_{18}H_{36}O_2$	19.4	284	2.58	19.4	284	0.61
10.	Isophytol	$C_{20}H_{40}O$	21.7	296	6.04	21.7	296	2.22
11.	Linolenic acid	$C_{18}H_{30}O_2$	22.3	278	8.39	22.6	278	18.06
12.	(9Z,12Z)-Ethyl octadeca-9,12-dienoate	$C_{20}H_{36}O_2$	22.9	308	1.45	-	-	-
13.	Ethyl 9,12, 15-0ctadecatrienoate	$C_{20}H_{34}O_2$	23.1	306	3.15	-	-	-
14.	1-Monolinolein	$C_{21}H_{38}O_4$	42.8	354	0.45	-	-	-
15.	1-Monolinolenoyl-rac-glycerol	$C_{21}H_{36}O_4$	42.9	352	1.32	-	-	-
16.	Heptacosane	$C_{27}H_{56}$	43.1	380	1.59	43.1	380	4.39
17.	(E,E,E,E)-Squalene	$C_{30}H_{50}$	44.6	410	19.26	44.6	410	28.29
18.	Heptacosane	$C_{27}H_{56}$	45.3	410	1.02	-	-	-
19.	1-Heptatriacotanol	$C_{37}H_{76}O$	45.6	536	1.88	-	-	-
20.	24,25-Dihydroxycholecalciferol	$C_{27}H_{44}O_3$	46.6	416	0.4	-	-	-
21.	Octacosyl Acetate	$C_{30}H_{60}O_2$	47	452	2.21	47.9	452	0.42
22.	Vitamin E	$C_{29}H_{50}O_2$	47.3	430	11.15	47.3	430	16.88
23.	Stigmasterol	$C_{29}H_{48}O$	48.4	412	1.52	48.4	412	0.8
24.	Clionasterol	$C_{29}H_{50}O$	48.9	414	1.62	49	414	0.7
25.	Silane, dimethyl(docosyloxy)butoxy-	$C_{28}H_{60}O_2Si$	50.1	456	15.2	-	-	-
26.	Androst-7-ene-6,17-dione, 2,3,14-trihydroxy-, (2beta,3beta,5alpha)-	$C_{19}H_{26}O_5$	52.6	334	9.75	-	-	-
27.	2,3-Dihydroxypropyl acetate	$C_5H_{10}O_4$	-	-	-	10	134	0.27
28.	Dihydroactinidiolide	$C_{11}H_{16}O_2$	-	-	-	14	180	0.28
29.	Fumaric acid, ethyl 2-methylallyl ester	$C_{10}H_{14}O_4$	-	-	-	14.4	198	0.19
30.	Phenol, 2-methyl-5-(1,2,2-trimethylcyclopentyl)-, (S)-	$C_{15}H_{22}O$	-	-	-	16.4	218	0.18
31.	Myristic acid	$C_{14}H_{28}O_2$	-	-	-	16.5	228	0.17
32.	1,5,9,9-Tetramethyl-spiro[3.5]nonan-5-ol	$C_{13}H_{24}O$	-	-	-	16.6	196	0.15
33.	3-Eicosyne	$C_{20}H_{38}$	-	-	-	17.3	278	0.62
34.	n-hexadecanoic acid	$C_{16}H_{32}O_2$	-	-	-	19	256	8.97
35.	Phytol	$C_{20}H_{40}O$	-	-	-	24.6	296	3.79
36.	Nonacosane	$C_{29}H_{60}$	-	-	-	45.3	408	2.14
37.	1,6,10,14,18,22-Tetracosahexaen-3-ol, 2,6,10,15,19,23-hexamethyl-, (all-E)-	$C_{30}H_{50}O$	-	-	-	45.6	426	1.39
38.	2,2,4-trimethyl-3-[(3E,7E,11E)-3,8,12,16-tetramethylheptadeca-3,7,11,15-tetraenyl]cyclohexan-1-ol	$C_{30}H_{52}O$	-	-	-	45.7	428	0.4
39.	2,2-dimethyl-3-(3,7,12,16,20-pentamethyl-3,7,11,15,19-heneicosapentaenyl)-,(all-E)-	$C_{30}H_{50}O$	-	-	-	46.2	426	0.38
40.	1,6,10,14,18,22-Tetracosahexaen-3-ol, 2,6,10,15,19,23-hexamethyl-, (all-E)-	$C_{30}H_{50}O$	-	-	-	46.3	426	0.39
41.	gamma-Tocopherol	$C_{28}H_{48}O_2$	-	-	-	46.6	416	0.66
42.	Hentriacontane	$C_{31}H_{64}$	-	-	-	47	436	1.56
43.	Stigmasta-5,22-dien-3-ol acetate	$C_{31}H_{50}O_2$	-	-	-	49.7	454	0.42
44.	Triacontyl acetate	$C_{32}H_{64}O_2$	-	-	-	49.9	480	0.65
45.	Stigmastan-3,5-diene	$C_{29}H_{48}$	-	-	-	50.4	396	0.7
46.	Ethyl iso-allocholate	$C_{26}H_{44}O_5$	-	-	-	52.6	436	0.57

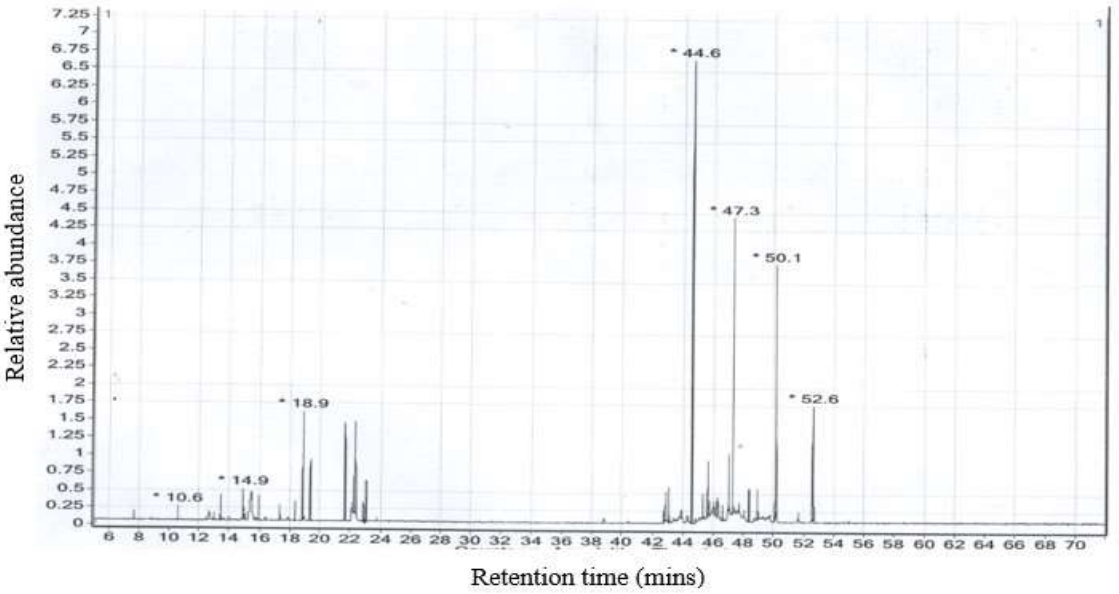

Figure 1: GC-MS chromatogram of *C. angustifolia* leaf ethanol extract.

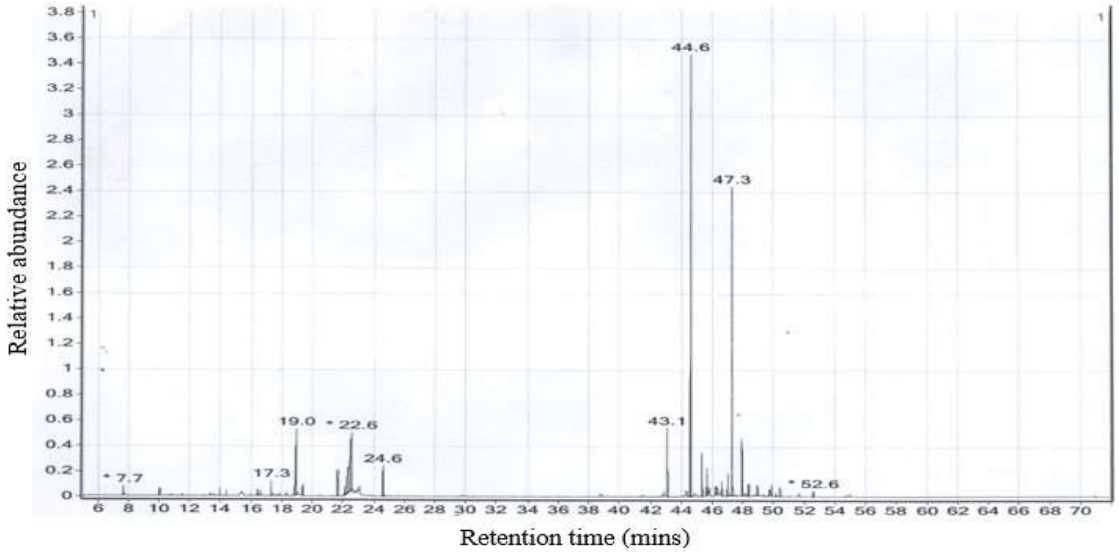

Figure 2: GC-MS Chromatogram of *C. angustifolia* leaf n-hexane extract

Plant extracts antiproliferative effects on HeLa and HEK-293T cell lines:

Cell cultures were established to evaluate the cytotoxic potential of CA extracts towards cervical cancer. As can be seen in Figure 3, ECA and HCA extracts affected cell growth very quickly; though, their increased activity was observed after 72 hrs. Data obtained from MTT assay absorbance revealed that ECA extract concentrations (10, 50, 100, 200, and 400 µg/mL) exhibited good activity in the cervical cancer cell line with IC_{50} =50 µg/mL and HCA extract displayed less effect with IC_{50} =76 µg/mL. However, HeLa cells showed consistently less effect at 10, 50, and 100 µg/mL and a significant effect at 200 and 400 µg/mL concentrations. Only 200 and 400 µg/mL concentrations showed statistically significant results when considering HCA extract. HEK-293T cells exhibited minimal or no response against both extracts, with IC_{50} = 245 µg/mL for ECA and IC_{50} =482 µg/mL for HCA. All tested concentrations of ECA and HCA extracts were compared with this study's mean absorbance of control (UT), which showed a statistically significant correlation. Cisplatin causes severe damage to cell growth and viability in cancerous as well as normal cells.

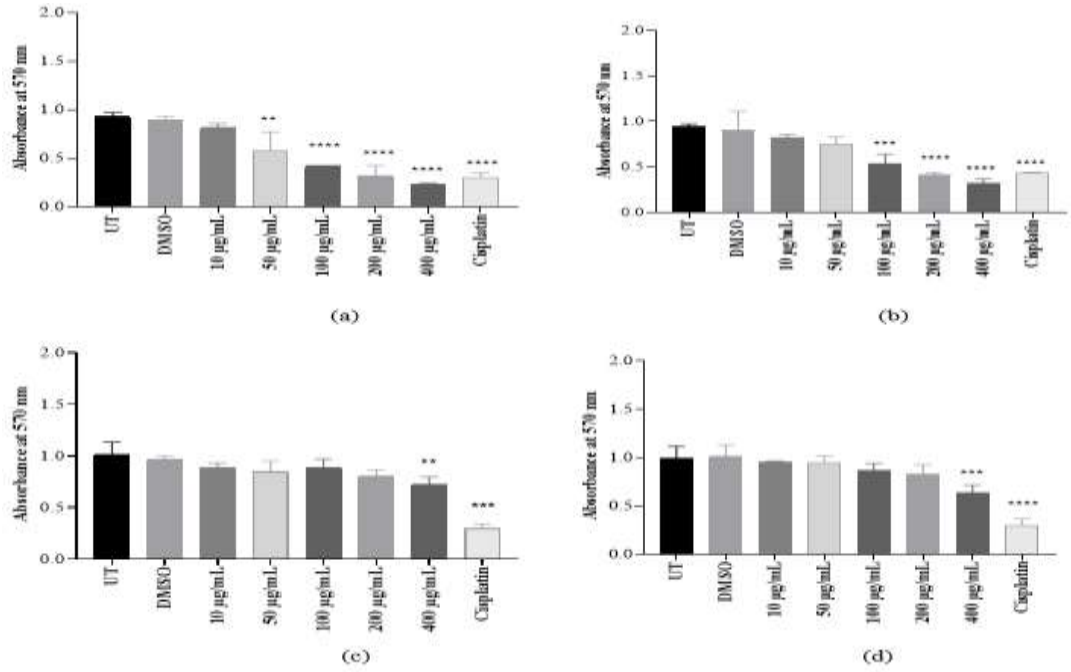

Figure 3: Graphical representation of the antiproliferative effect of *C. angustifolia* extracts on HeLa and HEK-293T cells (a) The ECA extract at 10, 50, 100, 200, and 400 µg/mL concentrations represented as bars from left to right evaluated by MTT assay, showed a remarkable decrease in cancer cells; (**b**) Antiproliferative activity of different dose-dependent concentrations of HCA extract exhibited reduced HeLa cells proliferation; **(c)** HEK-293T (noncancer) cell line response to ECA treatment showed very few effects; (**d**) HCA effect on healthy cell line also showed less or no activity. Cisplatin had strong inhibitory effects on both cell lines. The data is presented as absorbance means ± SD and compared with UT.

UT: Untreated**; DMSO:** Dimethyl sulfoxide; **ECA**: Ethanol extract of *C. angustifolia*; **HCA**: n-hexane extract of *C. angustifolia*

Cell viability analysis of plant extracts on HeLa and HEK-293T cell lines:

The crystal violet assay technique was used to quantify the remaining alive cells in treated culture media by assessing the dye absorbance of the cells at 570 nm of each well. It enters the cell cytoplasm and nucleus and is bound to only the proteins, RNA, and DNA molecules of alive cells. Cells that lose their permeability and undergo death exhibited less staining dye in the culture medium. For that purpose, the extract concentrations were further evaluated through crystal violet assay to approve the antiproliferative (MTT) activities of the extracts.

The percentage viability of HeLa and HEK-293T cells was determined by crystal violet assay (Figure 4). In crystal violet assay, ECA and HCA extracts showed a significant inhibitory effect on HeLa cells. Toxic effects of ECA extract revealed 88%, 76%, 53%, 51%, and 30%, and HCA showed 92%, 80%, 71%, 59%, and 47% of cell viability at 10, 50, 100, 200, and 400 µg/mL at 72 hrs. In this study, all results were compared with the percentage viability of the UT (100%) group, which showed a progressive decrease in a dose-dependent manner. The HEK-293T cell line proposed no harmful effects from either extract. The percentage viability was calculated as 92%, 88%, 84%, 77%, and 63% for ECA concentrations; however, 97%, 92%, 90%, 78%, and 63% for HCA concentrations. The viability % of cisplatin was calculated as < 42% in cancer cells and < 45 % in healthy control. Correlation between variables is measured by R-square in the data explained by the model. R square was calculated as (a) =0.9415, (b) =0.9539, (c) =0.9353, and (d) =0.9490, and *p*-value = < 0.05 for extracts.

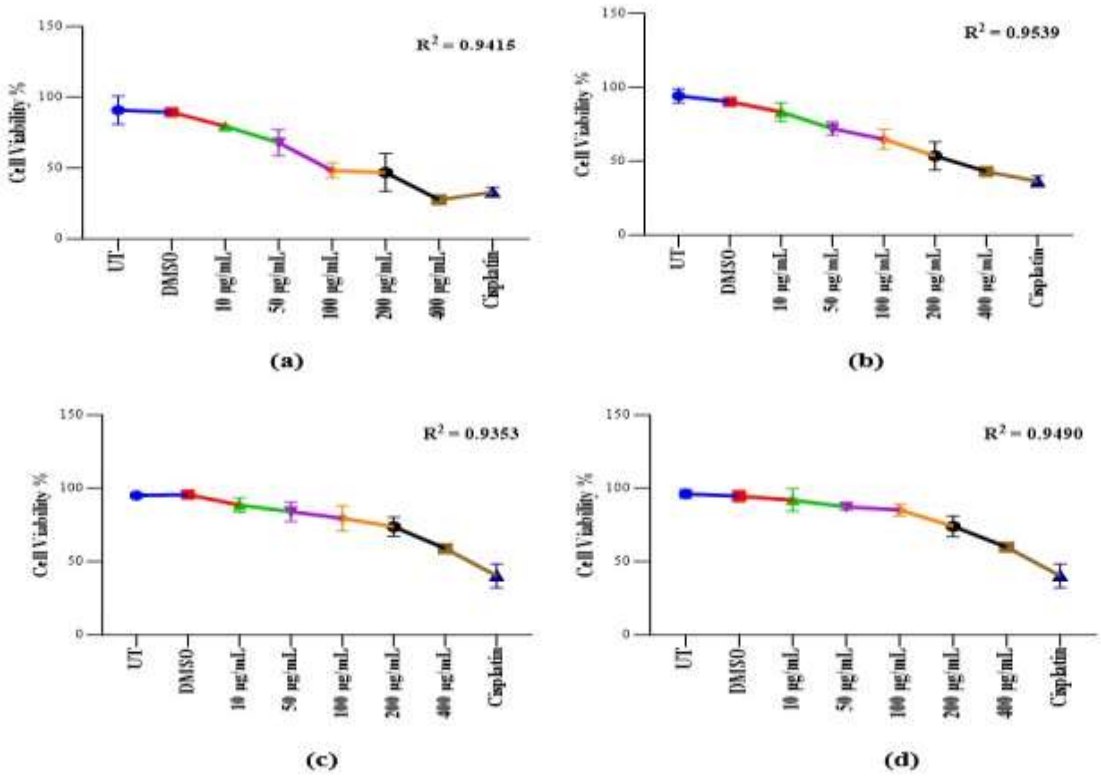

Figure 4: Cell viability analysis of *C. angustifolia* extracts on HeLa and HEK-293T cells (a) The viability of HeLa (cancer) cells was evaluated by the staining method represented as a trend-line slope. ECA extract concentrations exhibited a significant reduction in viability; (**b**) The HCA extract concentrations showed a prominent dose-dependent reduction in HeLa cells; (**c**) ECA extract on HEK-293T (noncancer) cells showed a slight fall in percentage viability; (**d**) HCA extract did not reveal severe toxicity on normal cells. All treatments differ significantly from the control group (UT) and are interpreted as $*p < 0.05$, $**p < 0.001$, $***p < 0.0001$. The results are described as percentage values.

UT: Untreated**; DMSO:** Dimethyl sulfoxide; **ECA**: Ethanol extract of *C. angustifolia*; **HCA**: n-hexane extract of *C. angustifolia*

Morphological examination of HeLa and HEK-293T cells treated with ethanol extract of *C. angustifolia*:

Morphological examination of HeLa and HEK-293T cells was done using an image station that revealed the change in shape and cytoplasmic condensation (Figure 5). A visible change in the morphology of HeLa cells was noticed at 72 hrs of incubation. No visibility of cell damage has been observed in healthy (HEK-293T) cells after exposure to ECA extract concentrations. These results support the assumption that ECA extract has antiproliferative potential against the growth and survival of cancer (HeLa) cells but does not affect normal (HEK-293T) cell growth. Notably, a noticeable difference was observed in the morphology of all groups, including UT, DMSO, ECA extract concentrations, and standard drug. Standard drug cisplatin disrupted cell-cycle regulation in normal and cancer cells by damaging DNA and cell membranes. In this study, cisplatin has been observed following the same mechanism on both cell lines.

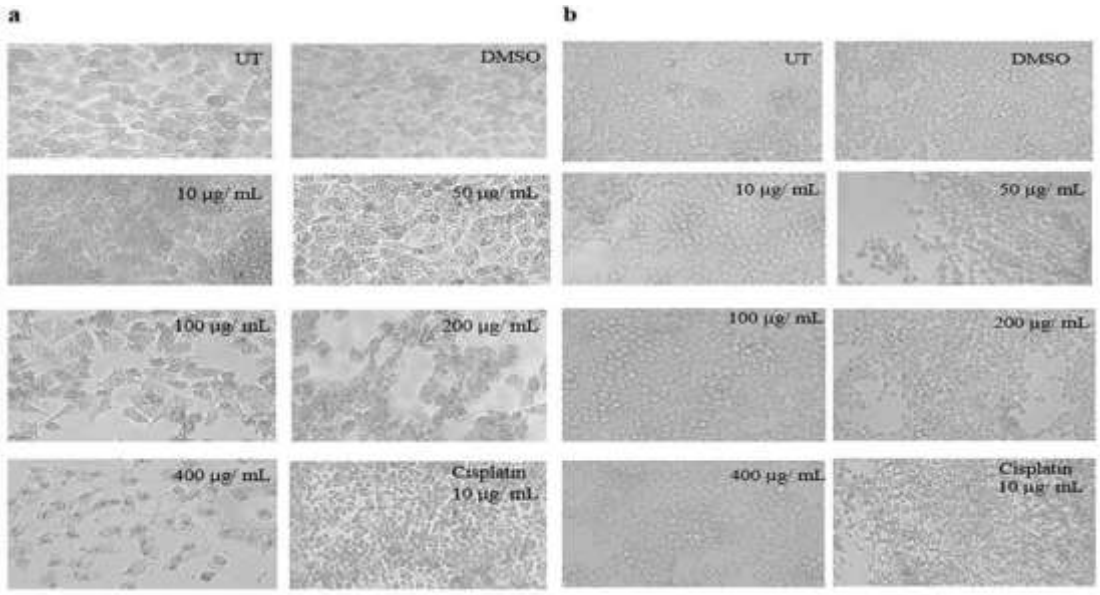

Figure 5: Morphological representation of HeLa and HEK-293T cells exposed to various concentrations of *C. angustifolia* ethanol extract (a) Morphological characteristics of HeLa (cancer) cells treated with different concentrations of ECA extract for 72 hrs; (**b**) HEK-293T (noncancer) cells represent normal morphology. Cisplatin revealed strong effects on both cell lines. All treated groups were compared with the untreated group.

UT: Untreated**; DMSO:** Dimethyl sulfoxide: **ECA**: Ethanol extract of *C. angustifolia*

Morphological examination of HeLa and HEK-293T cells treated with n-hexane extract of *C. angustifolia*:

HCA extract showed a less antiproliferative effect on HeLa cells (Figure 6). Thus, this study did not examine cytoplasmic condensation, irregular shape, or membrane damage at 10, 50, and 100 µg/mL, whether HCA extracts induced slight morphological changes at 200 and 400 µg/mL concentrations indicated antiproliferative effects on HeLa cells. HEK-293T also exhibited less change in morphology due to HCA extract, while cisplatin made disastrous changes in both cells.

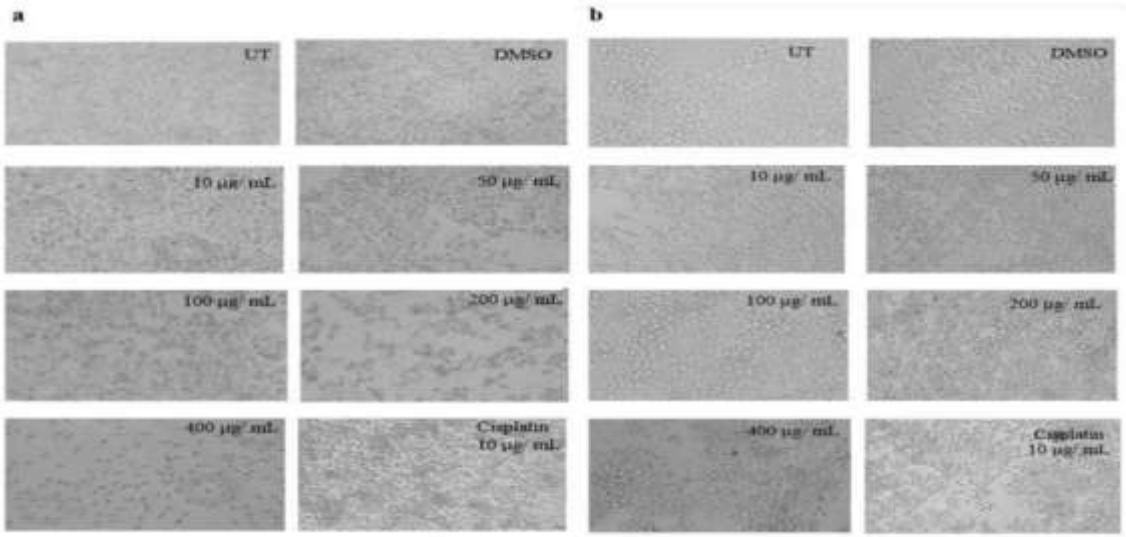

Figure 6: Morphological representation of HeLa and HEK-293T cells exposed to various concentrations of *C. angustifolia* n-hexane extract (a) Morphological assessment of HeLa (cancer) cells treated with various concentrations of HCA extract for 72 hrs; (**b**) HEK-293T (noncancer) cells displayed normal morphology at all concentrations of HCA extract. Cisplatin had severe effects on both cell lines. All treated groups were compared with the untreated control.

UT: Untreated**; DMSO:** Dimethyl sulfoxide; **HCA**: n-hexane extract of *C. angustifolia*

Effect of CA extract on expression levels of apoptotic proteins:

We examined the effect of the ethanol plant extract on the mRNA expression levels of apoptotic proteins (p53 and Bcl2) in treated and untreated samples of cervical cancer cells using real-time PCR. Differences in fold change of the HeLa expression were observed after being treated with the IC_{50} concentrations of ethanol extracts. These values were compared with the untreated (UT) sample and endogenous (*Hprt1*) control levels, denoted as a housekeeping gene, to normalize the mRNA levels among samples. Its expressions may vary slightly according to the condition and tissue/cell type. All the control and treated samples were analyzed by real-time PCR.

The HeLa cells showed noticeable upregulation of p53 in the control sample, with a mean Ct value of 20.0 in the untreated samples. As can be seen in Figure 7, HeLa cells show significant downregulation after being treated with the IC_{50} concentration. The fold change of 4.9 was calculated. The mRNA expression of the control samples of Bcl2 showed downregulation with a mean Ct value of 23.1 and upregulation of 20.0 in the HeLa cells after treatment. The fold change of 0.21 in HeLa cells was calculated. Bcl2 levels were slightly lower in the control sample than in the treated samples. Hprt1 is conventionally believed to be a housekeeping gene. In this study, Hprt1 expression compared to the control (< 0.05) reports a level with a mean Ct value range of 23-24 cycles. The expression profile of p53, Bcl2, and Hprt1 genes has been mentioned in Table 3. The bar graph representation of the fold change of p53, Bcl2, and Hprt1 analyzed by real-time PCR is presented in Figure 7.

	BCL2						**HPRT1**								
	Ct	**Min**	**Max**	**Range**	**SD**	**Mean**	**Ct**	**Min**	**Max**	**Range**	**SD**	**Mean**	**ΔCt.**	**ΔΔCt M-Value**	**fold-change**
CAS-HeLa-T	21.1 20 21	20	21.1	1.10	0.50	20.70	24 24.1 24.2	24.0	24.2	0.20	0.08	24.10	-3.40	**-2.23**	**0.21**
CAS-HeLa-C	22.5 23 24	22.5	24.00	1.50	0.62	23.17	24 25 24	24.0	25.0	1.0	0.47	24.33	-1.17		
	TP53						**HPRT1**								
CAS-HeLa-T	22 22.4 22	22.0	22.4	0.1	0.05	22.3	23 24.1 24	23.0	24.1	1.10	0.5	23.7	-1.3	**2.32**	**4.9**
CAS-HeLa-C	20 20 20	20	20	0.10	0.05	20.0	23 24 24.1	23.0	24.1	1.10	0.5	23.0	-3.6		

Table 3 Gene expression analysis of *TP53, Bcl-2,* and *HPRT1* genes by Real-time PCR
CAS: *Cassia angustifolia*; **HeLa:** Cervical cancer cell line; **T:** Treated samples; **C**: control samples

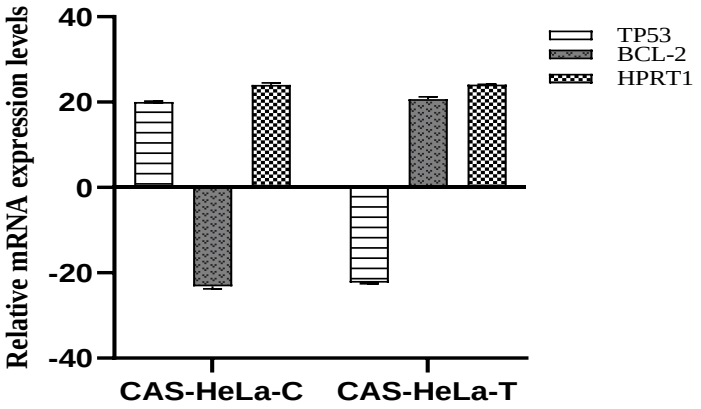

Figure 7: Graphical representation of mRNA expression analysis of *TP53, BCL2,* and *Hprt1* genes in HeLa cell lines. The graph shows the upregulation of *BCL2* and downregulation in levels of *P53* in HeLa cells after ECA treatment compared to the control (UT). Error bars show the

statistically significant correlation among groups with p = < 0.0001; *TP53*: Tumor suppressor gene; *BCL2*: B-cell lymphoma 2 protein; HeL: HeLa cell line.

Molecular Docking:

Selection of drug-like compounds for *In silico* analysis:

The compounds found to have several violations of Lipinski's criterion, as well as positive results for specific toxicological criteria, were not included in the present *in silico* analysis. Just four out of fifty-six compounds found by GCMS analysis were selected based on this criterion and interacted stably with oncoproteins. The physiochemical characteristics of ligand molecules that were screened using Lipinski's rule are displayed in Table 4.

TABLE 4: Lipinski's parameters and toxicity profiling of screened compounds from CA extracts

Ligands	MW	HBA	HBD	LogP	MR	L.V	Muta-Genicity	Carcinogenicity	Hepato-Toxicity	Acute oral toxicity
Phenol, 2-methyl-5-(1,2,2-trimethyl cyclopentyl)-, (S)-	218.33	1	1	4.03	69.55	Yes, 0 vio	None	None	No	III
7,9-Di-tert-butyl-1-oxaspiro[4.5]deca-6,9-diene-2,8-dione	276.37	0	3	3.40	79.66	Yes, 0 vio	None	None	No	III
Isophytol	296.53	1	1	6.18	98.98	Yes, 1 vio	None	None	No	III
1,5,9,9-Tetramethyl-spiro[3.5]nonan-5-ol	196.33	1	1	3.27	61.06	Yes, 0 vio	None	None	No	III

MW= Molecular weight: **MR=** Molar refractivity: **HBA**=Hydrogen bond acceptor: **HBD**=Hydrogen bond donor: **LV**= Lipinski's violation

Molecular interaction analysis:

Four ligands were used for each of the four target proteins using the docking criterion. Table 6 shows the binding energies in kcal/mol of these compounds. Figure 10 shows the 2D and 3D structures of protein-ligand interactions.

Table 5: Binding affinity of selected drug-like ligand molecules

Plant names	Receptors/ Proteins	Ligands	Affinity (kcal/mol)	Dist Rmsd l.b.	Best mode rmsd u.b.
Cassia angustifolia	p53	Phenol, 2-methyl-5-(1,2,2-trimethylcyclopentyl)-, (S)-	-7.5	0.000	0.000
	Bcl2	7,9-Di-tert-butyl-1-oxaspiro[4.5]deca-6,9-diene-2,8-dione	-6.8	0.000	0.000
	EGFR	Isophytol	-6.9	0.000	0.000
	HER2	1,5,9,9-Tetramethyl-spiro[3.5]nonan-5-ol	-5.0	0.000	0.000

RMSD= Root mean square deviation: **RMSD/lb**= Rmsd lower bond: **RMSD/ub**=: Rmsd upper bond

Residual interaction with the components of *C. angustifolia* extracts:

The 2D and 3D structures of target proteins and selected phytocompounds are illustrated in Figures 8 and 9, respectively. During molecular docking, the best-docked complexes were categorized based on the stable protein–ligand interactions with the preferably lower binding scores. The outcomes were predicted depending on the interactions and binding energies concerning ligands and cancer-related proteins. Using the program AutoDock vina, molecular docking was done to determine the stable binding conformations of various phytochemicals of the ECA and HCA extracts with target proteins, including p53, Bcl2, EGFR, and HER2. EGFR and HER2 are tyrosine kinase family receptors, p53 is tumor-suppressive protein and Bcl2 belongs to the antiapoptotic protein family. Four target proteins were docked with each drug-like phytochemical to ascertain their relative binding interactions. A total of six residual interactions were established between Phenol, 2-methyl-5-(1,2,2-

trimethylcyclopentyl)-, (S)- and P53, from which one hydrogen (Thr226) and the rest of the hydrophobic (Leu225/Trp237/Phe254/Pro260/Leu292) interactions. By the molecule 7,9-Di-tert-butyl-1-oxaspiro[4.5]deca-6,9-diene-2,8-dione forming eight interactions, namely Phe63/Tyr67/Tyr67/Asp70/Phe71/Val92/Leu96/ with Bcl2. It established hydrophobic contacts with active residues situated in the target protein's binding pocket. However, one hydrogen bond was generated by Isophytol with EGFR residue (Met793), and six amino acid residues, including Leu718/Val726/Leu777/Thr790/Thr854/Phe856, were involved in hydrophobic bond formation. Furthermore, 1,5,9,9-Tetramethyl-spiro[3.5] nonan-5-ol was another ligand that developed H-bond interaction with Arg434 residue. Moreover, one hydrophobic interaction was observed by Leu513 residue between ligand. Four test ligands for anticancer treatment have been chosen in the present research. Our goal was to learn more about the potential therapeutic evaluation of these selected compounds in treating CC. Phenol, 2-methyl-5-(1,2,2-trimethylcyclopentyl)-, (S)- had the highest binding affinity (-7.9 kcal/mol) with P53 among all tested substances. Although these chemicals were employed for the first time in a molecular interaction study, and said that they had significant anticancer activity. The illustrations of such interactions were generated and elaborated in Figure 10.

Figure 8: 3-Dimensional structures of cervical cancer-CC target proteins

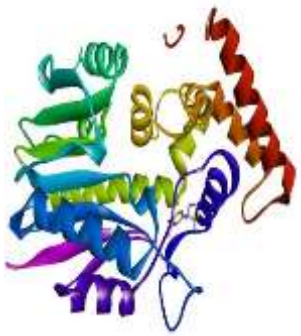	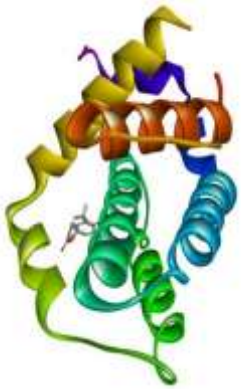	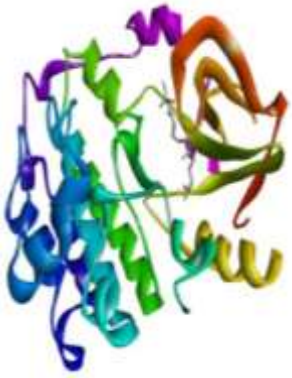	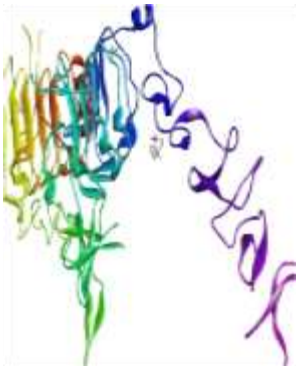
TP53:PDB ID: 2OCJ	BCL2:PDBID: 2W3L	EGFR:PDB ID:3poz	HER2: PDB ID:1n8z

Figure 9: 2-Dimensional configuration of screened compounds

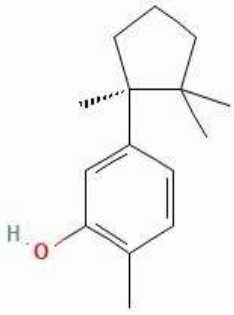	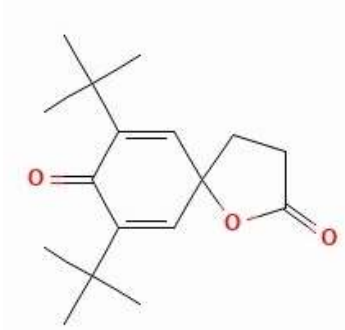	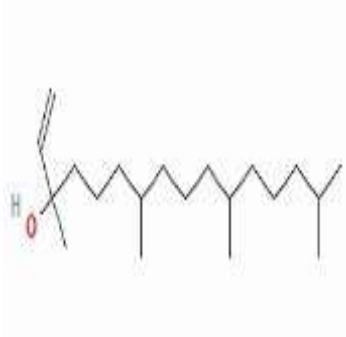	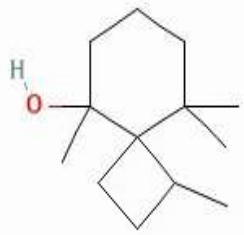
Phenol, 2-methyl-5-(1,2,2-trimethylcyclopentyl)-, (S)-	7,9-Di-tert-butyl-1-oxaspiro[4.5]deca-6,9-diene-2,8-dione	Isophytol	1,5,9,9-Tetramethyl-spiro[3.5]nonan-5-ol

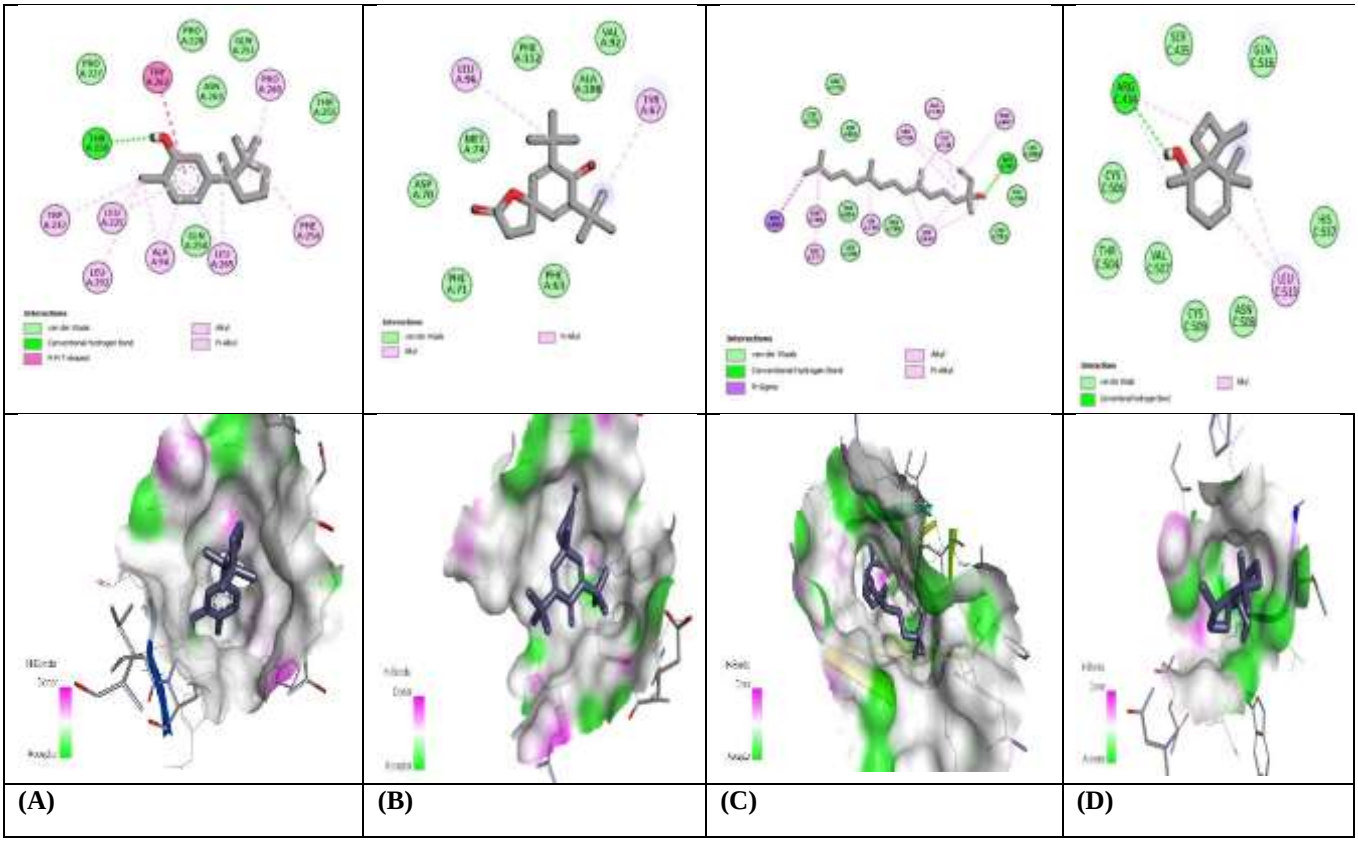

Figure 10: 2D and 3D interpretations of compounds: (A) Docking interpretation of p53 with Phenol, 2-methyl-5-(1,2,2-trimethylcyclopentyl)-,(S)-Crystal structure of p53 (PDB ID: 2OCJ); **(B)** Docking interpretation of Bcl2 protein with 7,9-Di-tert-butyl-1-oxaspiro[4.5]deca-6,9-diene-2,8-dione. Crystal structure of Bcl2 (PDB ID: 2W3L); **(C)** Docking interpretation of EGFR receptor with Isophytol. Crystal structure of EGFR (PDB ID: 3poz); **(D)** Docking interpretation of HER2 receptor with 1,5,9,9-Tetramethyl-spiro[3.5]nonan-5-ol. Crystal structure of HER2 (PDB ID: 1n8z)

Protein-ligand interaction:

The PLIP software was used to evaluate the interacting residues and their bond length in docked complexes (Table 6)

TABLE 6: The molecular interactions with amino acids of the protein.

Plant name	Proteins	Compounds name	Hydrogen interactions	Bond length	Hydrophobic interactions	Bond length
Cassia angustifolia	p53	Phenol,2-methyl-5-(1,2,2-trimethylcyclopentyl)-, (S)-	THR226	2.04	LEU225 TRP237 PHE254 PRO260 LEU292	3.63 3.93 3.95 3.96 3.45
	Bcl2	7,9-Di-tert-butyl-1-oxaspiro[4.5]deca-6,9-diene-2,8-dione	-	-	PHE63 TYR67 TYR67 ASP70 PHE71 VAL92 LEU96 ALA96	3.78 3.71 3.95 3.80 3.91 3.87 3.70 3.45
	EGFR	Isophytol	MET793	2.88	LEU718 VAL726 LEU777 THR790 THR854 PHE856	3.63 3.76 3.48 3.72 3.76 3.70
	HER2	1,5,9,9-Tetramethyl-spiro[3.5]nonan-5-ol	ARG434	2.28	LEU513	3.85

ADMET analysis of screened drug-like compounds:

Table 7 displays the comprehensive ADMET analysis of the top four compounds with the greatest hits. According to the literature review, the Ames test is significant, and a positive result suggests that the substance is mutagenic. Every chemical displayed a negative number, demonstrating its lack of mutagenicity. Among these substances, 1,5,9,9-Tetramethyl-spiro[3.5]nonan-5-ol showed the best absorption in the human gut, while 7,9-Di-tert-butyl oxaspiro[4.5]deca-6,9-diene-2,8-dione and isophytol had greater water solubility. For the P-gp substrate, isophytol and 1,5,9,9-Tetramethyl-spiro[3.5]nonan-5-ol compounds tested positive. Higher GI absorption was a feature shared by all the chosen compounds and crucial for medication absorption into the human body.

Additionally, it is anticipated that these substances will be able to cross the blood-brain barrier and may be useful in treating neurological conditions. No single molecule seems to be processed by CYP2C9, CYP2D6, and CYP3A4 during drug metabolism. It was discovered that three compounds, inhibited CYP1A2 but CYP2C19, CYP2C9, CYP2D6, and CYP3A4 were not inhibited by any of the compounds. No substance was found to have hepatotoxic or Ames toxicity. The phytochemicals had varying total clearance values. Of them, 7,9-Di-tert-butyl oxaspiro[4.5]deca-6,9-diene-2,8-dione had the lowest value, and the others showed the highest value removed from the plasma. These popular chemicals have a lot of promise for use as safe medication for both human and animal systems.

Table 7: Detailed ADMET prediction of screened compounds by admetSAR

Pharmacokinetic parameters	**Phenol, 2-methyl-5-(1,2,2-trimethyl cyclopentyl)-, (S)-**	**7,9-Di-tert-butyl oxaspiro[4.5]deca-6,9-diene-2,8-dione**	**Isophytol**	**1,5,9,9-Tetramethyl-spiro[3.5]nonan-5-ol**
Water solubility	-4.496	-3.26	-3.05	-1.905
Caco-permeability	1.607	0.8021	0.763	0.762
Human intestinal absorption	0.994	1.0000	0.9717	0.9904
Substrate of P-glycoprotein	No	No	Yes	Yes
BBB permeability	Yes	Yes	Yes	Yes
Gastrointestinal absorption	High	High	Yes	High
Inhibitor of CYP1A2	Yes	Yes	Yes	No
Inhibitor of CYP2C19	No	No	No	No
Inhibitor of CYP2C9	No	No	No	No
Inhibitor of CYP2D6	No	No	No	No
Inhibitor of CYP3A4	No	No	No	No
AMES test	No	No	No	No
Hepatotoxicity	No	No	No	No
Acute rat oral toxicity (LD50)	2.18	2.09	1.57	1.620
Drug plasma clearance	0.922	0.798	1.668	1.015

Discussion:

Healing with medicinal plants is as old as mankind itself. These treatments have demonstrated substantial therapeutic benefits in several domains, such as preventing cardiovascular ailments and possessing anti-inflammatory, anticancer, and antibacterial potential. Furthermore, the development of resistance to treatment for cancer has compelled researchers to look toward naturally occurring plant and marine compounds (Solowey *et al*., 2014). With this in mind, we thoroughly assessed the anticancer activities of CA plant leaf extracts on cervical cancer cell lines *in vitro* and *silico.*

The extraction and analysis of herbs are essential to the development of herbal compositions, including modernization and quality assurance. The GC-MS approach provides evidence for the qualitative and quantitative measures of bioactive components, as previously mentioned in our study (Kalsoom *et al*., 2023). The current research employed GC-MS to detect the substances contained in the leaf extracts and showed the existence of steroids, phenols, flavonoids, fatty acids, and terpenes. In total, 26 and 30 phytochemicals were found in the ECA and HCA extracts by GC-MS. We will discuss the biological and pharmaceutical activities of those compounds here identified with more area percentages. The significant components in the ECA extract were triterpene-like squalene (19.26%), a precursor of non-steroidal cholesterol. According to Purkiewicz et al. (2022), it is produced as acetyl-CoA, a metabolic intermediate with antioxidant, anticancer, and anti-atherosclerotic qualities. The essential polyunsaturated omega-3 fatty acid linolenic acid (8.39%), dimethyl(docosyloxy)butoxy-(15.2%), octacosyl acetate (11.15%), androst-7-ene-6,17-dione, 2,3,14-trihydroxy-, (2beta, 3beta,5alpha)-(9.75%), and silane are all involved in the biosynthesis of

hormone-like eicosanoids that regulate immune function and inflammation (Mariamenatu and Abdu, 2021). In human gastric adenocarcinoma (AGS) cells, phytol (6.04%), a diterpene acyclic alcohol that promotes apoptosis and autophagy, causes an accumulation of acidic vesicles and downregulates the Akt, p70S6K, and mTOR (mechanistic target of rapamycin) pathways (Islam *et al*., 2018). In addition to having antibacterial, anti-fibrinolytic, anti-inflammatory, antioxidant, hemolytic, metabolic, and anticancer properties in a variety of tumor types, palmitic acid (6.03%) functions as 5-an alpha-reductase inhibitor implicated in the progress of prostate cancer (CaP) (Zhu *et al*., 2021). It confirms that the phytocompounds in plant ECA extract, which are useful for treating many illnesses, are present, as the GC-MS study clearly shows. The main bioactive substances were found in the following amounts according to the HCA extract results: squalene (20.29%), linolenic acid (18.06%), vitamin E (16.88%), heptacosane (4.39%), and phytol (3.79%). Isoamyl acetate, ethyl palmitate, phytol, linolenic acid, heptacosane, 1-Heptatriacotanol, (E,E,E,E)-Squalene, Octacosyl Acetate, stigmasterol, and cholesterol were among the 30 phytocompounds that were detected in both extracts.

Therefore, finding innovative treatment or medication options that will selectively target cancer cells while not affecting healthy cells is desperately needed (Nelson *et al*., 2020). Here, we investigated the anticancer potential of *Cassia angustifolia* extracts against HEK-293T noncancer cells and HeLa cervical cancer cells. HeLa cells were then selected for additional research based on their sensitivity to HCA and ECA extracts. Significantly, the toxicity of ECA to cancer cells was better understood after MTT and crystal violet experiments revealed its relative nontoxicity to normal cells. Previous research on *C. angustifolia* extracts' cytotoxicity relied on the MTT colorimetric test utilizing the MTT calorimetric test. Ahmed and colleagues determined the IC_{50} and cell viability at 100, 150, 200, and 250 µg/µL against cancer (MCF-7, HeLa, and HepG2) and normal (HCEC) cell lines. In HepG2 cells, ethanol concentrations demonstrated 28% viability with an IC_{50} of 7.28 µg/µL. In HeLa cells, methanol showed 33% viability with an IC_{50} of 5.45 µg/µL, and in MCF-7 cells, 43% viability with an IC_{50} of 4 µg/µL. According to Ahmed et al. (2016), noncancer (HCEC) cells showed 100% vitality toward both extracts (Ahmed *et al*., 2016). The findings of this study revealed that the antiproliferative activity of ECA and HCA inhibited succinate dehydrogenase enzyme activity, which is in charge of turning MTT dye into insoluble formazan crystals, and more efficiently repressed the growth of cancer cells at IC_{50} = 50 µg/mL of ECA and IC_{50} = 76 µg/mL of HCA (Figure 3).

After being treated for 72 hours with ECA and HCA extracts, the proportion of viable HeLa cells was considerably reduced (Figure 4). At 10, 50, 100, 200, and 400 µg/mL doses, the antiproliferative effects of ECA extract were shown to be 88%, 76%, 53%, 51%, and 30%, whereas the effects of HCA extract were 92%, 80%, 71%, 59%, and 47% cell viability. A considerably lower (30%) viability percentage was attained at an ECA concentration of 400 µg/mL. For ECA, the visibility of HEK-293T cells was 92%, 88%, 84%, 77%, and 63%; for HCA extract, it was 97%, 92%, 90%, 78%, and 63%. The HEK-293T cell line towards extract saw less or no negative effects. The percentage viability of the control UT (Untreated, 100%) cells was compared to all of the findings.

In cancer (HeLa) cells, the ECA and HCA extracts caused morphological alterations such as membrane blebbing, chromatin condensation, DNA breakage, apoptotic body formation, and cell shrinkage (Figures 5 and 6). The study found that the extracts had distinct anticancer action against cancer (HeLa) cells as opposed to non-cancerous (HEK-293T) cells. By blocking DNA replication and cell division, cisplatin inhibits the propagation of both types of cells. The morphological evaluation of HeLa cells following treatment with *Cassia fistula* CaFH fraction was reported by Kaur et al. By looking for blebbing and nuclear margination (moderate apoptosis), they were able to confirm the activation of apoptosis and growth inhibition (Kaur *et al*., 2020). In this investigation, treated HeLa cells displayed a statistically significant ($P < 0.05$) difference, suggesting that *C. angustifolia* has an apoptogenic impact that varies with dosage and time.

Modulation of oncogenes is one of the most common genetic abnormalities found in a variety of human malignancies. More than half of all cancers in humans are caused by *TP53* gene mutations. Numerous genes, including those related to apoptosis, have been demonstrated to be transcriptionally regulated by the transcriptional activator TP53 (Graur *et al*., 2016). Mutations in the TP53 cause the

synthesis of genetically unstable cells and interfere with its ability to normally control cell proliferation, leading to ineffective DNA repair and, eventually, the formation of neoplasia (Sadia *et al*., 2020). Apoptosis is known to be regulated by the *BCL2* gene, which encodes a cellular protein that inhibits apoptosis in normal cells (Entezari and Sheikhan *et al*., 2018). The current study aimed to examine how *BCL2* and *TP53*, two oncogenes, were expressed differently in HeLa cervical carcinoma. Variations in the fold change of certain gene mRNA expression levels in cancer cell lines treated with ethanol extract IC_{50} values have been noted. According to the current work, *C. angustifolia* regulates TP53 and BCL2 signaling to cause apoptosis in cervical (HeLa) cancer cells. It has been reported that control samples of the cervical cancer cell line exhibit upregulated TP53 and downregulated BCL2. The current study's real-time PCR analysis revealed that when HeLa cells were treated with an IC_{50} dose of ECA extract, there was a regulation in the mRNA expression of the apoptosis-related genes *BCL2* and *TP53*.

TP53 is a tumor suppressor gene protein that interacts with *BCL2* to encourage apoptosis. Salam et al. (2020) state that the interaction between BCL2 and P53 suppresses the inhibitory effect on BAX, releases cytochrome C, and ultimately results in apoptosis. A missense mutation in TP53 affects the nuclear buildup of the p53, which is exhibited as overexpressed in immunohistochemistry, as seen in other investigations. P53 positivity is seen in 17–45% of all histological categories of endometrial carcinomas. Nakamura et al. (2019) reported that type-II endometrial cancer had a high percentage of p53 expression, ranging from 30 to 86%, whereas type-I endometrial cancer had a p53-positive rate of 10 to 44%. We compare the housekeeping gene (Hprt1)'s mRNA expression levels in treated (IC50) and untreated (control) samples. In both samples, steady expression of Hprt1 was detected, with a Ct value ranging from 23 to 24 cycles. Table 2 includes information on the expression profile of the *TP53*, *BCL2*, and *Hprt1* genes. Consequently, it is suggested that treatment with ECA extract causes cells to die in a way that is dependent on apoptosis, suggesting that this might be a useful therapeutic option for the treatment of cancer. Furthermore, in HepG2, HeLa, Huh7, MCF-7, and MDA-MB-231, *ACTB*, *B2M*, *HPRT1*, *UBC*, and *YWHAZ* were among the five stable genes when rated using the geNorm, NormFinder, and RefFinder algorithms (Gorji-Bahri *et al*., 2021).

By learning more about how phytochemicals interact with targets to inhibit or stimulate enzymatic signaling to treat a certain ailment, scientists may successfully create innovative substitute medicines (Kiran *et al*., 2023). The current investigation screened drug-like compounds by adhering to Lipinski's guidelines and meeting toxicological requirements. Beyond these boundaries, a molecule may lose valuable absorption, metabolism, distribution, and excretion characteristics, making it unlikely to be studied further as a medication. Based on these constraints, only four of the fifty-six chemicals found in both extracts were physiologically active. After screening from the medicinal plant *Cassia*, these ligands were discovered to have strong affinity with the Bcl-2, EGFR, P53, and HER2 antiapoptotic proteins/receptors under investigation. Using *in silico* molecular docking studies, we were able to estimate the amino acid residues and protein-ligand binding energies involved in the interactions. One important regulator in the intrinsic mitochondrial apoptotic pathway is Bcl-2. As a recognized target in apoptosis, the intrinsic mitochondrial apoptotic pathway is often inhibited by Bcl-2 (Singh *et al*., 2018). According to a prior study, ABT-199's control over Bcl-2 in its hydrophobic pocket enhanced anticancer efficacy *in vivo* and cell death *in vitro* (Cang *et al*., 2015). Anonymuricin A, muricatocin A, annohexocin, muricatocin A/B, and annomuricin-D-one are bioactive compounds from *A. muricata* L. that, according to a molecular docking reported by Antony and Vijayan, showed high docking scores with alternative antiapoptotic protein, Bcl-Xl (Rosdi *et al*., 2018).

The bioactive compounds from the ECA and HCA extracts (phenol, 2-methyl-5-(1,2,2-trimethylcyclopentyl)-,(S)-, 7,9-Di-tert-butyl-1-oxaspiro[4.5]deca-6,9-diene-2,8-dione, isophytol, and 1,5,9,9-Tetramethyl-spiro[3.5]nonan-5-ol) showed good binding affinities (-7.5, 6.8, -6.9, and -5.0 kcal/mol) on interaction with P53, Bcl2, EGFR, and HER2 proteins (Table 5). As a result, we demonstrated that antiapoptotic proteins (P53 and Bcl2) also showed a good binding interaction. The interacting amino acid residues involved in various molecular interactions are given in Table 6. As a

result, these best-hit biomolecules from the two *C. angustifolia* extracts demonstrated good anticancer capabilities, defining their potential for use in developing multiple-targeted antitumor medicines.

Conclusion:

The key objective of the current investigation was to demonstrate the significant cytotoxic properties of leaf extracts from *C. angustifolia*. Both extracts showed better outcomes and were subjected to GCMS analysis to identify the pharmacologically active phytocompounds. Fifty-six compounds were filtered, among them, only 4 were selected following the criteria of drug-likeness and showing no sign of toxicity using various *in-silico* software. Four of these compounds demonstrated the greatest hits with the following target macromolecules: phenol, 2-methyl-5-(1,2,2-trimethylcyclopentyl)-,(S)-,7,9-Di-tert-butyl-1-oxaspiro[4.5]deca-6,9-diene 2,8-dione, isophytol, and 1,5,9,9-Tetramethyl-spiro[3.5]nonan-5-ol. As far as we know, most of the biological activities of *C. angustifolia* are supported by well-established expression analysis and molecular docking investigation. As a result, this plant, particularly its ethanol extract, has a great deal of promise to become a targeted, nontoxic, and efficient drug for preventing and treating cervical cancer. More *in vivo* research is needed to validate the anticancer effect of novel drug formulations by investigating various underlying molecular processes.

Conflict of interest

The authors declare no conflicts of interest.

Acknowledgments

The authors express their gratitude to ….....

Author contributions

AK wrote the manuscript draft, designed the protocol, applied the method, and collected the data; AA revised the manuscript and supervised the project; TM and SA supervised and facilitated and provided necessary cell culture lab supervision; SA revised the manuscript; HS supervised and facilitated the gene expression analysis; MS Investigation, and editing; AK analyzed molecular docking interpretations. All authors read and approved the final manuscript.

Funding

……

References:

1. Abhilashi, K., Rani, J., Kumari, P., Kumari, S., Choudhary, V., and Pankaj, S. (2023). Association of p-53 and Bcl-2 Expression with HPV Genotyping in Cervical Carcinoma: A Tertiary Care Centre Experience. *Indian Journal of Gynecologic Oncology*, *21*(1), 8.
2. Ahmed, S. I., Hayat, M. Q., Tahir, M., Mansoor, Q., Ismail, M., Keck, K., and Bates, R. B. (2016). Pharmacologically active flavonoids from the anticancer, antioxidant and antimicrobial extracts of Cassia angustifolia Vahl. *BioMed Central complementary and alternative medicine*, 16(1): 1-9.
3. Aung, T. N., Qu, Z., Kortschak, R. D., and Adelson, D. L. (2017). Understanding the effectiveness of natural compound mixtures in cancer through their molecular mode of action. *International journal of molecular sciences*, *18*(3), 656.
4. Baeshen NA, Albeshri AO, Baeshen NN, Attar R, Karkashan A, Abbas B, Baeshen MN (2022). In silico screening of some compounds derived from the desert medicinal plant Rhazya stricta for the potential treatment of COVID-19. Sci. Rep 12(1): 11120. https://doi.org/10.1038/s41598-022-15288-2
5. Cang, S., Iragavarapu, C., Savooji, J., Song, Y., and Liu, D. (2015). ABT-199 (venetoclax) and BCL-2 inhibitors in clinical development. *Journal of hematology & oncology*, *8*(1), 1-8.

6. Çankaya N, Azarkan SY, Tanış E (2022). The molecular interaction of human anti-apoptotic proteins and in silico ADMET, drug-likeness and toxicity computation of N-cyclohexylmethacry lamide. *Drug Chem. Toxicol* 45(5), 1963-1970. https://doi.org/10.1080/01480545.2021.1894711
7. Entezari, M., and Sheikhan, S. (2018). Evaluation of Bcl2 gene expression in MCF-7 Human Breast Cancer Cells under treatment of Centaurea Behen extract and Cisplatin. *Archives of Advances in Biosciences*, 9(4): 11-16.
8. Ezzat, S. M., Shouman, S. A., Elkhoely, A., Attia, Y. M., Elsesy, M. S., El Senousy, A. S., & El Tanbouly, N. (2018). Anticancer potentiality of lignan-rich fraction of six Flaxseed cultivars. *Scientific Reports*, *8*(1), 544.
9. Federico, C., Sun, J., Muz, B., Alhallak, K., Cosper, P. F., Muhammad, N., and Azab, A. K. (2021). Localized delivery of cisplatin to cervical cancer improves its therapeutic efficacy and minimizes its side effect profile. *International Journal of Radiation Oncology* Biology* Physics*, *109*(5), 1483-1494.
10. Gorji-Bahri, G., Moradtabrizi, N., and Hashemi, A. (2021). Uncovering the stability status of the reputed reference genes in breast and hepatic cancer cell lines. *Plos one*, 16(11): e0259669.
11. Graur, F., Furcea, L., Mois, E., Biliuta, A., Rozs, A. T., Negrean, V., and Al Hajjar, N. (2016). Analysis of p53 Protein Expression in Hepatocellular Carcinoma. *Journal of Gastrointestinal and Liver Diseases*, 25(3).
12. He, M., Xia, L., and Li, J. (2021). Potential mechanisms of plant-derived natural products in the treatment of cervical cancer. *Biomolecules*, *11*(10), 1539.
13. Islam, M. T., Ali, E. S., Uddin, S. J., Shaw, S., Islam, M. A., Ahmed, M. I., and Atanasov, A. G. (2018). Phytol: A review of biomedical activities. *Food and chemical toxicology*, 121: 82-94.
14. Kalsoom, A., Altaf, A., Jilani, M. I., Sattar, H., Maqbool, T., and Muhammad, T. (202). In vitro antiproliferative potential of Cassia angustifolia extracts on HepG2 cells to combat liver cancer. *International Journal of Applied and Experimental Biology*.
15. Kaur, S., Pandit, K., Chandel, M., and Kaur, S. (2020). Antiproliferative and apoptogenic effects of Cassia fistula L. n-hexane fraction against human cervical cancer (HeLa) cells. *Environmental Science and Pollution Research*, 27(25): 32017-32033.
16. Kikuchi, H. Yuan, B. Hu, X and Okazaki, M. Chemopreventive and anticancer activity of flavonoids and its possibility for clinical use by combining with conventional chemotherapeutic agents. *American Journal of Cancer Research,* 2019, *9*, 1517–1535.
17. Kiran, A., Altaf, A., Sarwar, M., Malik, A., Maqbool, T., and Ali, Q. (2023). Phytochemical profiling and cytotoxic potential of Arnebia nobilis root extracts against hepatocellular carcinoma using in-vitro and in-silico approaches. *Scientific Reports*, *13*(1), 11376.
18. Kumari, S., Singh, A., Sangal, R., and Sharma, N. R. (2021). KAP study on cervical cancer and human papillomavirus vaccine acceptability among adolescent girls of Eastern UP: a cross sectional study. *International Journal of Reproduction, Contraception, Obstetrics and Gynecology*, *10*(5), 2031-2036.
19. Lipinski, C.A., Lombardo, F., Dominy, B.W., Feeney, P.J., 1997. Experimental and computational approaches to estimate solubility and permeability in drug discovery and development settings. *Advance Drug Delivery Reviews*, 23 (1–3), 3–25.
20. Mariamenatu, A. H., and Abdu, E. M. (2021). Overconsumption of omega-6 polyunsaturated fatty acids (PUFAs) versus deficiency of omega-3 PUFAs in modern-day diets: the disturbing factor for their "balanced antagonistic metabolic functions" in the human body. *Journal of Lipids*, 1-15.
21. Masuku, N. P., and Lebelo, S. L. (2019). Investigation of the effects of Kigelia africana (Lam.) Benth. Extracts on TM3 Leydig cells. *Asian Journal of Pharmacuetical and Clinical Research*, 12(10): 87-92.
22. Mbugua, R. W., Njagi, E. M., Ngule, C. M., and Mwitari, P. (2019). Gene expression mediated antiproliferative potential and safety of selected medicinal plants against cancerous and normal cells. *BioRxiv*, 578948.

23. Mendie LE, and Hemalatha S (2022). Molecular docking of phytochemicals targeting GFRs as therapeutic sites for cancer: An in silico study. *Applied Biochemistry and Biotechnology*, 1-17 (194): 215–231. https://doi.org/10.1007/s12010-021--03791-7
24. Mohamad Rosdi, M. N., Mohd Arif, S., Abu Bakar, M. H., Razali, S. A., Mohamed Zulkifli, R., and Ya'akob, H. (2018). Molecular docking studies of bioactive compounds from Annona muricata Linn as potential inhibitors for Bcl-2, Bcl-w and Mcl-1 antiapoptotic proteins. *Apoptosis*, *23*, 27-40.
25. Momtazi-Borojeni, A. A., Ghasemi, F., Hesari, A., Majeed, M., Caraglia, M., and Sahebkar, A. (2018). Anticancer and radio-sensitizing effects of curcumin in nasopharyngeal carcinoma. *Current pharmaceutical design*, *24*(19), 2121-2128.
26. Morris, J. L., Gillet, G., Prudent, J., and Popgeorgiev, N. (2021). Bcl-2 family of proteins in the control of mitochondrial calcium signalling: an old chap with new roles. *International Journal of Molecular Sciences*, *22*(7), 3730.
27. Nakamura, M., Obata, T., Daikoku, T., and Fujiwara, H. (2019). The association and significance of p53 in gynecologic cancers: the potential of targeted therapy. *International Journal of Molecular Sciences*, *20*(21), 5482
28. Nawaz, A., Jamal, A., Arif, A., and Parveen, Z. (2021). In vitro cytotoxic potential of Solanum nigrum against human cancer cell lines. *Saudi Journal of Biological Sciences*, 28(8), 4786-4792.
29. Nelson, V. K., Sahoo, N. K., Sahu, M., Sudhan, H. H., Pullaiah, C. P., and Muralikrishna, K. S. (2020). In vitro anticancer activity of Eclipta alba whole plant extract on colon cancer cell HCT-116. *BMC complementary medicine and therapies*, *20*, 1-8.
30. Ouyang, L.; Luo, Y.; Tian, M.; Zhang, S.-Y.; Lu, R.; Wang, J.-H.; Kasimu, R.; Li, X. Plant natural products: From traditional compounds to new emerging drugs in cancer therapy. *Cell Proliferation.* 2014, *47*, 506–515.
31. Park, S. H., Kim, M., Lee, S., Jung, W., and Kim, B. (2021). Therapeutic potential of natural products in treatment of cervical cancer: a review. *Nutrients*, *13*(1), 154.
32. Pillaiyar, T., Meenakshisundaram, S., and Manickam, M. (2020). Recent discovery and development of inhibitors targeting coronaviruses. *Drug discovery today*, *25*(4), 668-688.
33. Purkiewicz, A., Czaplicki, S., and Pietrzak-Fiećko, R. (2022). The Occurrence of Squalene in Human Milk and Infant Formula. *International Journal of Environmental Research and Public Health*, 19(19): 12928.
34. Ravindranath PA, Forli S, Goodsell DS, Olson AJ, Sanner MF (2015). AutoDockFR: advances in protein-ligand docking with explicitly specified binding site flexibility. *PLoS Computional Biology*, 11(12): e1004586. https://doi.org/10.1371/journal.pcbi.1004586
35. Sadia, H., Bhinder, M. A., Irshad, A., Zahid, B., Ahmed, R., Ashiq, S., and Akbar, A. (2020). Determination of expression profile of p53 gene in different grades of breast cancer tissues by real time PCR. *African Health Sciences*, 20(3): 1273-1282.
36. Salam, H. S., Tawfik, M. M., Elnagar, M. R., Mohammed, H. A., Zarka, M. A., and Awad, N. S. (2022). Potential Apoptotic Activities of Hylocereus undatus Peel and Pulp Extracts in MCF-7 and Caco-2 Cancer Cell Lines. *Plants*, 11(17): 2192.
37. Sattar H, Firyal S, Awan AR, Habib-ur-Rehman, Tayyab M, Hasni SM, Ali MM, Saeed S, Mehmood T, Aqib IA, Khan HM, Wasim M (2021). Genetic Association of Polymorphism and Relative mRNA Expression of Tumor Necrosis Factor-Alpha Gene in Mastitis in Sahiwal Cows. *International Journal of Agricultural and Biological Engineering*, 25:701–708. https://doi.org/10.17957/IJAB/15.1719
38. Shivanika C, Kumar D, Ragunathan V, Tiwari P, Sumitha A (2020). Molecular docking, validation, dynamics simulations, and pharmacokinetic prediction of natural compounds against the SARS-CoV-2 main-protease. *Journal of Biomolecular Structure and Dynamics.* https://doi.org/10.1080/07391102. 2020.1815584
39. Singh, R., Letai, A., and Sarosiek, K. (2019). Regulation of apoptosis in health and disease: the balancing act of BCL-2 family proteins. *Nature reviews Molecular cell biology*, *20*(3), 175-193.

40. Solowey, E., Lichtenstein, M., Sallon, S., Paavilainen, H., Solowey, E., and Lorberboum-Galski, H. (2014). Evaluating medicinal plants for anticancer activity. *The Scientific World Journal*, *2014*.
41. Sultana T, Mitra AK, and Das S (2022). Evaluation of the anticancer potential of Excoecaria agallocha (L.) leaf extract on human cervical cancer (SiHa) cell line and assessing the underlying mechanism of action. *Future journal of Pharmaceutical Sciences,* 8(1): https://doi.org/10.1186/s43094-021-00389-y
42. Sun, C, Brown, A. J., Jhingran, A., Frumovitz, M., Ramondetta, L., and Bodurka, D. C. (2014). Patient preferences for side effects associated with cervical cancer treatment. *International journal of gynecological cancer: official journal of the International Gynecological Cancer Society*, *24*(6), 1077.
43. Sung, H., Ferlay, J., Siegel, R. L., Laversanne, M., Soerjomataram, I., Jemal, A., and Bray, F. (2021). Global cancer statistics 2020: GLOBOCAN estimates of incidence and mortality worldwide for 36 cancers in 185 countries. *CA: a cancer journal for clinicians*, *71*(3), 209-249.
44. Tulashie, S. K., Adjei, F., Abraham, J., and Addo, E. (2021). Potential of neem extracts as natural insecticide against fall armyworm (Spodoptera frugiperda (JE Smith)(Lepidoptera: Noctuidae). *Case Studies in Chemical and Environmental Engineering*, *4*, 100130.
45. Umar HI, Siraj B, Ajayi A, Jimoh TO, and Chukwuemeka PO (2021). Molecular docking studies of some selected gallic acid derivatives against five non-structural proteins of novel coronavirus. *Journal of Genetic Engineering and Biotechnology,* 19(1): https://doi.org/10.1186/s43141-021-00120-7
46. Umesh HR, Ramesh KV, and Devaraju KS. Molecular docking studies of phytochemicals against trehalose-6-phosphate phosphatases of pathogenic microbes. *Beni-Suef University Journal of Basic and Applied Sciences,* 2020;*9*(1):1–14. doi: 10.1186/s43088-019-0028-6
47. Zhu, S., Jiao, W., Xu, Y., Hou, L., Li, H., Shao, J., and Kong, D. (2021). Palmitic acid inhibits prostate cancer cell proliferation and metastasis by suppressing the PI3K/Akt pathway. *Life Sciences*, 286: 120046.